

Indirect search of Heavy Neutral Leptons using the DUNE Near Detector

S. Carbajal and A.M. Gago

Sección Física, Departamento de Ciencias, Pontificia Universidad Católica del Perú, Apartado 1761, Lima, Perú

We evaluate the potential of the DUNE Near Detector (DUNEND) for establishing bounds for heavy neutral leptons in the region of masses below 500 MeV. These bounds are obtained from the deficit of muon and electron charged current events expected at the LArTPC of DUNEND. The latter happens because the active neutrinos produced from the decays of the heavy ones do not hit the detector. As a result, we get limits of $|U_{\mu 4}|^2 < 4 \times 10^{-2} (7 \times 10^{-5})$ and $|U_{e 4}|^2 < 1.5 \times 10^{-2} (1 \times 10^{-4})$ for masses below 10 MeV, five years per each mode (neutrino/antineutrino) and for a 5%(0%) overall normalization uncertainty in neutrino charged current event rates prediction. These limits, within the region of masses below 2(10) MeV, are better than those that can be achieved by DUNE direct searches for the case of a 5%(0%) uncertainty. We can also impose limits on $|U_{\mu 4}|^2$ in a mass region free of constraints (100 eV - 1 MeV). For masses below 1 MeV, we improve the current experimental constraints by up to 2 orders of magnitude when no uncertainties are considered. However, when a 5% uncertainty is present, our limits can only improve current constraints on $|U_{e 4}|^2$ by up to a factor of 6.

I. INTRODUCTION

Heavy neutral leptons (HNLs) are singlet (right-handed) fermions states introduced for explaining the non-zero neutrino masses, interacting, via Yukawa coupling, with the Higgs boson and the leptonic doublet, a Dirac mass term, and also appearing in the Majorana mass term. The nearly sterile states that arise after the diagonalization of the mass terms mentioned before interact with matter via suppressed mixing to the active neutrinos of the Standard Model (SM) [1, 2].

The HNLs are candidates to solve important particle physics and cosmology issues [1]. They can help explain the smallness of the active neutrino masses via the See-saw mechanism [3], act as possible dark matter candidates [4] and also explain the baryon asymmetry of the universe through their role in leptogenesis (see [1, 5] and references therein). On the other hand, neutrino oscillations involving light sterile states have been proposed to explain the excess of electron antineutrino and neutrino events at LSND and MiniBoone, respectively, as well as the deficit of electron antineutrino events at reactor experiments [6]. The HNL masses required for solving the before mentioned problems fall within a mass range that spans from keV to TeV. As a consequence of their relevance, there have been several HNL searches in this wide mass range, placing limits on the possible values of the HNL mass m_N and its mixing to the SM neutrinos $|U_{\alpha 4}|^2$ [2, 7].

In particular, searches of HNLs in the range of masses of 1-400 MeV have been conducted in accelerator-based experiments through searches for low-energy peaks in the energy spectrum of the muons resulting from pion ($\pi^\pm \rightarrow \mu^\pm \nu_H$) and kaon decays ($K^\pm \rightarrow \mu^\pm \nu_H$) [8-11]. With no positive results found so far, they obtain upper bounds for $|U_{\mu 4}|^2$ such as 10^{-6} for $m_N \sim 10$ MeV and 10^{-9} for $m_N \sim 300$ MeV.

This work aims to assess the sensitivity of the DUNE experiment in setting upper limits for $|U_{\mu 4}|^2$ and $|U_{e 4}|^2$ for masses below 500 MeV. We achieved the latter

by measuring a deficit of neutrino charged current (ν CC) events at the DUNE Near Detector (DUNEND) [12]. This deficit of CC events comes from those active neutrinos that are born from HNLs and have angular distributions spanned outside the detector coverage. We consider the decrease in CC events as an indirect signal of HNLs and use it to set limits on the mixing parameters. Additionally, we present an analysis of the possibility of finding confidence regions for the values of $(m_N, |U_{\alpha 4}|^2)$ if a deficit of CC events is found at DUNE [13].

This paper goes as follows: in the second section we discuss the theoretical framework of HNL production and decay. Then, in the third one, we describe the experimental setup. In the fourth section, the details of our simulation are given. While, in the fifth one, our results are presented. We draw our conclusions in the final section.

II. THEORETICAL FRAMEWORK

As we already mentioned, the nearly sterile mass eigenstates couple to the active flavor states via an extended version of the Pontecorvo-Maki-Nakagawa matrix (PMNS) [14], which can be expressed as follows:

$$\nu_\alpha = \sum_{i=1,2,3} U_{\alpha i} \nu_i + U_{\alpha 4} N, \quad (1)$$

where N represents the HNL field. It is also helpful to write the new active neutrino flavor states in terms of the flavor states of the SM ν_α^{SM} , which represent the neutrino flavor states when the values of the 3×3 PMNS mixing matrix are assumed. This can be done by the approximation [15]

$$\nu_\alpha \approx \nu_\alpha^{\text{SM}} \left(1 - \frac{|U_{\alpha 4}|^2}{2} \right) + U_{\alpha 4} N. \quad (2)$$

Due to the connection above, the HNLs can be produced in any weak decay involving active neutrinos. The

production rate of HNLs depends kinematically on its mass m_N , the strength of its mixing to active neutrinos $|U_{\alpha 4}|^2$ and the nature of the decaying particle that produces it, which, from now on, we will refer to as its parent. In this work, we are interested in HNLs with masses below the kaon mass (m_K). The production of HNLs from kaon and pion decays, followed by the muon decays, dominate at the typical energies of beam dump experiments such as DUNE. Their production from heavier particles, such as D mesons or τ leptons, is also possible, but it is rare since the production of the latter is heavily suppressed in comparison to the light mesons. Table I shows the dominant HNL production channels from light leptons and mesons, along with the maximum kinematically allowed values of the masses for the HNLs. A rough estimation of these values is obtained by subtracting the total rest mass of the particles produced, other than the HNLs, from the corresponding mass of their parent particle.

TABLE I. Channels considered for the production of HNLs. The maximum possible value of m_N is shown for each channel. Charged conjugate channels were also considered.

Channel	m_N (MeV)	Channel	m_N (MeV)
$\mu^+ \rightarrow e^+ \nu_e \bar{\nu}_\mu$	105.14	$K^+ \rightarrow \mu^+ \nu_\mu$	387.81
$\pi^+ \rightarrow \mu^+ \nu_\mu$	33.91	$\pi^0 e^+ \nu_e$	358.19
$e^+ \nu_e$	139.06	$\pi^0 \mu^+ \nu_\mu$	253.04
$K_L^0 \rightarrow \pi^\pm e^\mp \nu_e$	357.12	$e^+ \nu_e$	493.17
$\pi^\pm \mu^\mp \nu_\mu$	252.38		

We calculated the branching ratios for HNL production by using the formulas from Ref. [16]. For instance, Fig. 1 shows the branching ratios of the dominant HNL production channels below the kaon mass for $|U_{\mu 4}|^2 = 1$. We can note that almost all the branching ratios decrease with m_N , with the only exception being the leptonic decays of charged kaons, $K^\pm \rightarrow N\mu^\pm$. Above 34 MeV, the production from pions is kinematically forbidden; this is important since this means that all heavy neutral leptons above this mass will be produced only from kaon decays. As the value of m_N increases, the branching ratio of $K^\pm \rightarrow N\mu^\pm$ keeps increasing as well, surpassing the branching ratios of $K^\pm \rightarrow N\pi^0\mu^\pm$ at around 80 MeV and of $K_L^0 \rightarrow N\pi^0\mu^\pm$ at around 160 MeV. Finally, the branching ratio of $K^\pm \rightarrow N\mu^\pm$ reaches its maximum at around 260 MeV and then decreases until it is kinematically forbidden. The endpoint of each branching ratio corresponds to the maximum m_N given in Table I.

The production of HNLs via semileptonic decays involves hadronic currents that cannot be calculated from first principles due to the non-perturbative nature of QCD at low energies. Therefore, the dynamics of these decays are modeled by form factors that represent the momentum distribution of the quarks inside the mesons and parametrize the momentum transfer between the hadronic current and the lepton pair [17]. For all the

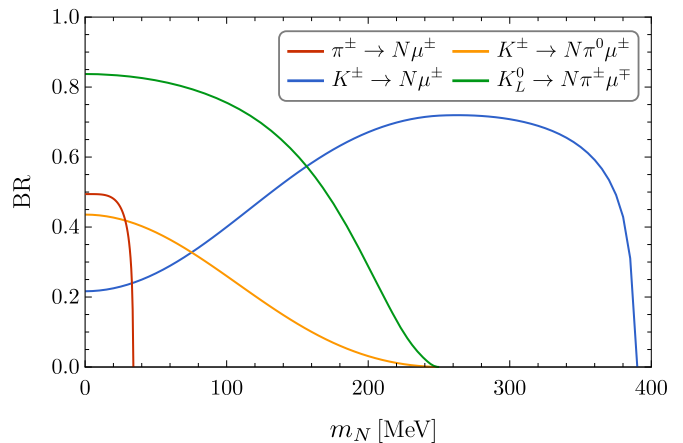


FIG. 1. Branching ratios of the dominant HNL production channels for $|U_{\mu 4}|^2 = 1$.

semileptonic decays in Table I, we used the form factors presented in [16].

After their production, all the HNLs propagate and then decay on flight via mixing with active neutrinos. Table II shows all the decay channels for the HNLs considered in this work. We included all the kinematically allowed decays to final states involving pseudoscalar mesons as well as pure leptonic decays for $m_N < m_K$. A more complete table can be found in [18].

TABLE II. HNL decay channels considered in this work. The minimum required value of m_N is shown for each channel.

Channel	Threshold [MeV]	Channel	Threshold [MeV]
$\nu\nu\nu$	10^{-9}	$e^\mp \pi^\pm$	140.08
$\nu e^+ e^-$	1.02	$\nu \mu^+ \mu^-$	211.32
$\nu e^\pm \mu^\mp$	106.17	$\mu^\mp \pi^\pm$	245.23
$\nu \pi^0$	134.98	$e^\mp K^\pm$	494.19

The partial width of a HNL decay channel involving a final lepton l_α or light neutrino ν_α is directly proportional to the mixing parameter squared $|U_{\alpha 4}|^2$. Therefore, the total width and lifetime of the HNLs also depend on the relevant mixing parameters. The lifetime dependence on the values of $|U_{\alpha 4}|^2$ can have a huge impact on the position of the decay vertex of the HNL and hence on its possible signal at a detector. Setting small values for the $|U_{\alpha 4}|^2$ means that the HNLs are being produced at a lower rate, but, at the same time, that these HNLs have a greater lifetime and therefore decay further away from the detector.

When we determine the individual partial widths of each channel, there is a factor of two that differentiates between the decays of Dirac and Majorana HNLs [18]. For instance, a Dirac HNL can decay to charged pions

only via $N \rightarrow e^- \pi^+$, while a Majorana one can also decay through $N \rightarrow e^+ \pi^-$. This evidently has an effect on the rates of π^+/π^- production from HNL decays but does not affect the partial decay widths. This means that CC mediated channels have the same partial widths for Dirac and Majorana neutrinos:

$$\begin{aligned}\Gamma(N_M \rightarrow l^- X^+) &= \Gamma(N_D \rightarrow l^- X^+), \\ \Gamma(N_M \rightarrow l^+ X^-) &= \Gamma(\bar{N}_D \rightarrow l^+ X^-).\end{aligned}\quad (3)$$

On the other hand, NC mediated channels do distinguish between Dirac and Majorana HNLs. This is because the contractions of the NC operator add an additional contribution to the differential decay width of the Majorana HNLs [18, 19],

$$d\Gamma(N_M \rightarrow \nu X) = d\Gamma(N_D \rightarrow \nu X) + d\Gamma(\bar{N}_D \rightarrow \bar{\nu} X). \quad (4)$$

Therefore, a factor of two appears when comparing the partial widths of NC mediated decays,

$$\Gamma(N_M \rightarrow \nu X) = 2\Gamma(N_D \rightarrow \nu X). \quad (5)$$

Equations (3) and (5) imply that the total widths (Γ_T) of Majorana and Dirac HNLs are related by

$$\Gamma_T(N_M) = 2\Gamma_T(N_D), \quad (6)$$

which translates into a difference between their lifetimes,

$$\tau(N_M) = \frac{1}{2}\tau(N_D). \quad (7)$$

For very low masses ($m_N \ll m_e$), the factor of two in Eq. (5) disappears [20], making the total widths and lifetimes of Dirac and Majorana HNLs indistinguishable. Part of the mass range that we will explore in this work falls in the region of very low masses.

At the end of this section, we will describe how the active neutrinos flux is affected by the production of HNLs. For this purpose, we will show how the SM parent meson's branching ratios are modified when the production of HNL occurs. Let us start by defining the SM total decay rate of the pion (Γ_π^{SM}):

$$\Gamma_\pi^{\text{SM}} = \Gamma^{\text{SM}}(\pi \rightarrow e\nu_e) + \Gamma^{\text{SM}}(\pi \rightarrow \mu\nu_\mu), \quad (8)$$

and the decay rate with heavy neutral leptons (Γ_π^{BSM}):

$$\begin{aligned}\Gamma_\pi^{\text{BSM}} &= \Gamma^{\text{BSM}}(\pi \rightarrow e\nu_e) + \Gamma^{\text{BSM}}(\pi \rightarrow \mu\nu_\mu) + \Gamma(\pi \rightarrow NX) \\ &\approx \Gamma^{\text{SM}}(\pi \rightarrow e\nu_e) \left(1 - \frac{|U_{e4}|^2}{2}\right) \\ &\quad + \Gamma^{\text{SM}}(\pi \rightarrow \mu\nu_\mu) \left(1 - \frac{|U_{\mu4}|^2}{2}\right) \\ &\quad + \Gamma(\pi \rightarrow NX).\end{aligned}\quad (9)$$

The branching ratio of ν_μ production from pion decays in the presence of HNLs can then be written as

$$\begin{aligned}\text{BR}^{\text{BSM}}(\pi \rightarrow \mu\nu_\mu) &= \frac{\Gamma^{\text{BSM}}(\pi \rightarrow \mu\nu_\mu)}{\Gamma_\pi^{\text{BSM}}} \\ &\approx \frac{\Gamma^{\text{SM}}(\pi \rightarrow \mu\nu_\mu) \left(1 - \frac{|U_{\mu4}|^2}{2}\right)}{\Gamma_\pi^{\text{SM}}} \cdot \frac{\Gamma_\pi^{\text{SM}}}{\Gamma_\pi^{\text{BSM}}} \\ &\approx \frac{\Gamma^{\text{SM}}(\pi \rightarrow \mu\nu_\mu)}{\Gamma_\pi^{\text{SM}}} \cdot \frac{\Gamma_\pi^{\text{SM}}}{\Gamma_\pi^{\text{BSM}}} \left(1 - \frac{|U_{\mu4}|^2}{2}\right) \\ &\approx \text{BR}^{\text{SM}}(\pi \rightarrow \mu\nu_\mu) \cdot \frac{\Gamma_\pi^{\text{SM}}}{\Gamma_\pi^{\text{BSM}}} \left(1 - \frac{|U_{\mu4}|^2}{2}\right).\end{aligned}\quad (10)$$

A similar relation can be found for the branching ratio of ν_e production from pion decays:

$$\text{BR}^{\text{BSM}}(\pi \rightarrow e\nu_e) \approx \text{BR}^{\text{SM}}(\pi \rightarrow e\nu_e) \cdot \frac{\Gamma_\pi^{\text{SM}}}{\Gamma_\pi^{\text{BSM}}} \left(1 - \frac{|U_{e4}|^2}{2}\right), \quad (11)$$

where $\text{BR}^{\text{SM}}(\pi \rightarrow \mu(e)\nu_{\mu(e)})$ represents the branching ratio of $\nu_\mu(\nu_e)$ production from pion decays in the SM. We can see that the introduction of HNLs causes the production of either muon or electron neutrinos from pions to be suppressed by the factor

$$\mathcal{K}_\pi^\alpha(m_N, |U_{\alpha4}|^2) = \frac{\Gamma_\pi^{\text{SM}}}{\Gamma_\pi^{\text{BSM}}} \left(1 - \frac{|U_{\alpha4}|^2}{2}\right), \quad (12)$$

with $\alpha = e, \mu$. Fig. 2 illustrates the dependence on m_N of the factor \mathcal{K}^μ for several parents assuming $|U_{\mu4}|^2 = 10^{-4}$. For each meson, the suppression factor acts only up to a maximum HNL mass due to kinematical constraints, which are the same constraints shown in Table I and Fig. 1. Although the effect is small, the high luminosity of DUNE makes it possible to use this effect to set limits on the heavy neutral leptons parameters.

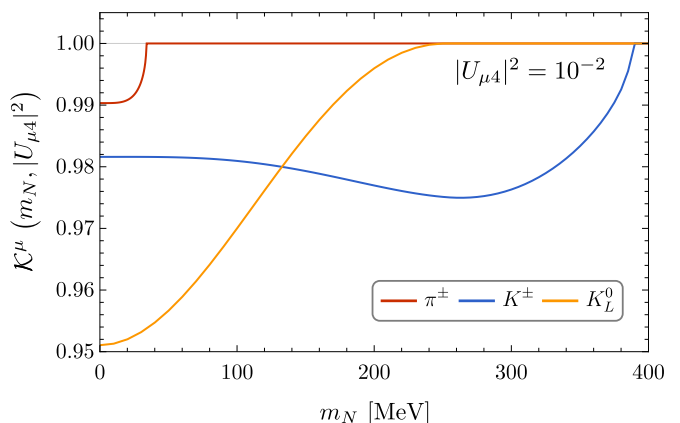


FIG. 2. Suppression factor $\mathcal{K}^\mu(m_N, |U_{\mu4}|^2 = 10^{-4})$ of muon neutrino production as a function of m_N .

Thus, each particle capable of producing active neutrinos can produce HNLs, leading to a suppression of the

former. The latter happens even when only one mixing $|U_{\alpha 4}|^2$ is turned on. In fact, we can see from Eqs. (10) and (11) that, if we turn off either one of the mixings $|U_{\alpha 4}|^2$, the production of the active neutrinos of flavor α is still suppressed by the factor $\Gamma_{\pi}^{\text{SM}}/\Gamma_{\pi}^{\text{BSM}}$. As we will show further ahead, the reduction in the active neutrino flux would imply the possibility that they do not reach the DUNE, decreasing the number of expected CC events at this facility.

III. EXPERIMENTAL SETUP

In order to simulate how the presence of HNLs affects the number of ν CC events at DUNE, we based our experimental setup in the DUNE Near Detector, described in Ref. [13].

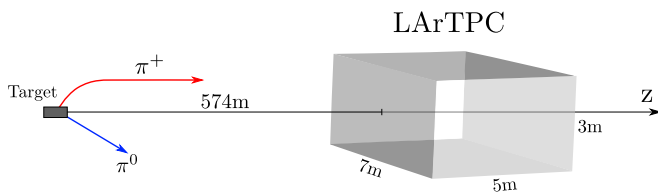


FIG. 3. Experimental setup for the LArTPC in neutrino mode (not to scale). Charged particles are deflected by the magnetic horns.

We assume that the LBNF-DUNE beam collides protons with 120 GeV of energy into a graphite target, producing 1.47×10^{21} POTs per year. At each collision, several mesons are produced, including mostly pions, kaons and charmed mesons.

The muons and long-lived charged mesons (π^{\pm} and K^{\pm}) produced are deflected by focusing magnetic horns located right after the target; as a consequence, their trajectories end up preferably oriented along the beam axis, as shown schematically in Fig. 3. On the other hand, the trajectories of neutral mesons (D^0 , K_L^0 and π^0), tau leptons and short-lived charged heavy mesons (D^{\pm} and D_s^{\pm}) are not affected by the focusing horns. Most particles decay in flight inside the decay pipe, a cylinder with a length of 230 m and a diameter of 2 m; however, a small number of long-lived particles reach the end of the decay pipe and decay at rest at the decay pipe's surface.

The Near Detector Liquid Argon Time Projection Chamber (LArTPC) is located at 574 m from the target. It has the shape of a parallelepiped with width and height (both transverse to the beam direction) of 7 m and 3 m, respectively, and a length of 5 m in the beam direction. The LArTPC is filled with a fiducial mass of 50 tons of liquid Argon. There is also the Multi-Purpose Detector (MPD), which is a magnetic spectrometer designed to study particles exiting the LArTPC that contains a one-ton high-pressure cylindrical gaseous argon time projection chamber. Since we are interested in the

effects of HNLs on the ν CC events at the DUNE Near Detector, we will not take into account the MPD in our simulation setup because its impact on our results is negligible.

We take also into account the possibility of moving the detectors to several off-axis positions along the x-axis, a setup known as DUNE-PRISM [21].

IV. SIMULATION ROUTE FOR HNLs

A. Parents Production

For the simulation of the production of HNLs from light mesons, we used the data provided by the DUNE Beam Interface Working Group (BIWG) [22], which makes use of GEANT4 [23, 24] and FLUKA [25, 26]. This data includes information about the decay positions and momenta of pions, kaons and muons after they exit the focusing horns. The most abundant light parent in DUNE is the pion, followed by kaons and finally muons, as can be seen in Fig. 4. In this work we will consider that the neutrino CC event rates might have an overall normalization uncertainty of up to 5% due to uncertainties in the modeling of production of mesons and leptons at the DUNE target and neutrino cross sections. We encapsulate this uncertainty by a parameter σ_a that varies from 0 to 0.05. Setting $\sigma_a = 0$ is equivalent to assume that there are no uncertainties in the DUNE neutrino CC event rates and, for a systematic uncertainty of 5%, σ_a takes the value of 0.05.

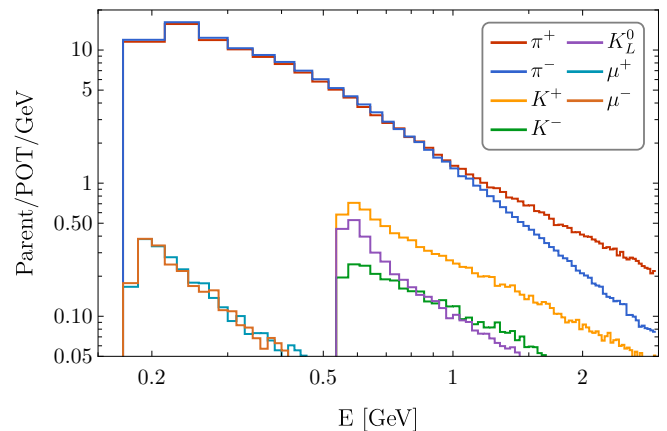


FIG. 4. Spectra of light particles capable of producing HNLs in the DUNE beam. Different bin widths have been used for different particles.

The production of HNLs from heavier particles such as D mesons and τ leptons is also possible, but it is expected to have a negligible effect on the active neutrino flux, which is totally dominated by production from lighter mesons. In order to test the relevance of HNL production from these heavy particles, we used PYTHIA8 [27] to estimate the neutrino flux generated by D^0 , \bar{D}^0 , D^{\pm} , D_s^{\pm}

and τ^\pm at DUNE. We observed that these heavy parents do not contribute significantly to the DUNE neutrino flux and hence the production of HNLs coming from them will have a negligible effect on the number of CC events. Consequently, our analysis is restricted only to the production of HNLs from light mesons and muons.

B. Production of HNLs

The production and decay chain of a HNL will depend on its mass, the mass of its parent, the nature of its parent (lepton, scalar meson or vector meson), the parent decay channel, the HNL nature (Dirac or Majorana), the HNL decay channel and the value of the mixing parameter involved. In principle, we could turn on, simultaneously, the three mixing parameters $|U_{\alpha 4}|^2$, $\alpha = e, \mu$ and τ ; however, in our analysis we will consider only one non-zero mixing parameter at a time.

Given a HNL mass and nature, we gave PYTHIA8 the kinematic information of the parents and let it handle the kinematics of all the HNL production and decay chain, up to final active neutrinos. As expected, the HNL production and decay channels are weighted with their corresponding branching ratios.

In Fig. 5 we show the number of HNLs produced at DUNE from mesons decays in one year and in neutrino mode for $|U_{\mu 4}|^2 = 10^{-4}$. Production from pion decays dominates at low masses, followed by charged and neutral kaons. The spectrum endpoint for pions and kaons corresponds to the maximum allowed m_N displayed in Table I when they decay into muons. For completeness, we also present the production from charmed mesons, which, as expected, is comparatively smaller and completely overshadowed for masses below 387.81 MeV. Above this threshold, HNL production from pions and kaons is kinematically forbidden, and the contribution from charmed meson decays dominates. This contribution is several orders of magnitude smaller than the one from light mesons, as we already claimed.

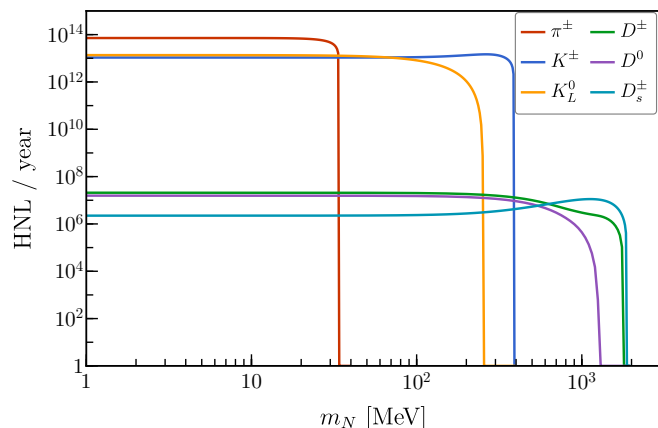


FIG. 5. Heavy Neutral leptons produced from mesons in one year in neutrino mode for $|U_{\mu 4}|^2 = 10^{-4}$.

C. Decay of HNL - Active Neutrinos

We focus on the active neutrinos produced from the HNL decays. We are interested in differentiating the number of these neutrinos that fall within the detector's geometrical acceptance from those outside of it. With this aim, we parametrize the probability that an active neutrino hits the detector by two distances along the HNL propagation axis. These distances represent two different decay vertices of the HNL and are calculated considering the geometrical coverage of the detector and the kinematical information provided by PYTHIA8, which depends on its lifetime, production vertex, velocity and the direction of propagation of the active neutrino. The aforementioned probability is given by:

$$w(d_1, d_2) = \exp\left(-\frac{d_1}{v\gamma\tau_0}\right) - \exp\left(-\frac{d_2}{v\gamma\tau_0}\right), \quad (13)$$

where v is the HNL's velocity, γ its Lorentz factor and τ_0 its proper lifetime.

For illustrative purposes, we present in Fig. 6 the scheme of the explained above, for the case when the HNL moves along the beam axis. It is clear that our analysis is general and takes into account the tridimensional shape of the LArTPC and all the possible ways in which an active neutrino might enter the detector, including cases where the HNL is outside the detector coverage.

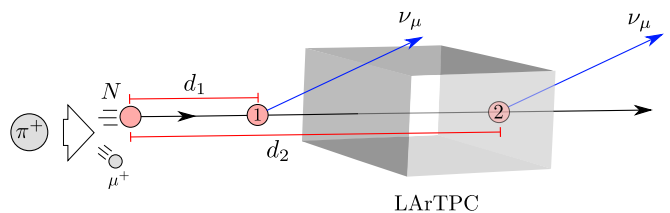


FIG. 6. A HNL N propagates and decays into an active neutrino ν_μ . If the HNL decays between positions 1 and 2, the active neutrino ν_μ hits the LArTPC.

It is important to mention that when we deactivate the HNL production, we reproduce the (pure SM) active neutrino fluxes arriving at the LArTPC predicted by the DUNE Collaboration [28].

In Fig. 7 we display the average HNLs' decay positions measured from the target and projected along the Z-axis for $|U_{\mu 4}|^2 = 10^{-4}$ and $|U_{\mu 4}|^2 = 10^{-1}$ and for Dirac and Majorana HNLs. The dotted line represents the position of the LArTPC, which is located at $z = 574$ m. Given that the lifetime of the HNL is inversely proportional to $|U_{\mu 4}|^2$, we can see that, as long as the mixing decreases, the average decay positions at Z increase. In the mass range we studied, for $|U_{\mu 4}|^2 = 10^{-4}$, on average, all the HNLs decay behind the LArTPC; hence, one active neutrino is lost in the DUNE flux at the LArTPC per each HNL produced. On the other hand, for $|U_{\mu 4}|^2 = 10^{-1}$, the average HNL decay position coincides

with the LArTPC location at $m_N \approx 255$ MeV, which implies that, above this mass, the HNLs decay mainly before the detector.

We also note that in both cases there is a small increase in the average decay positions around 30 MeV. This happens because the production of HNLs from pion decays becomes kinematically forbidden around this energy and decays from kaons start to dominate. This makes the average HNL more energetic and therefore it can travel larger distances before decaying.

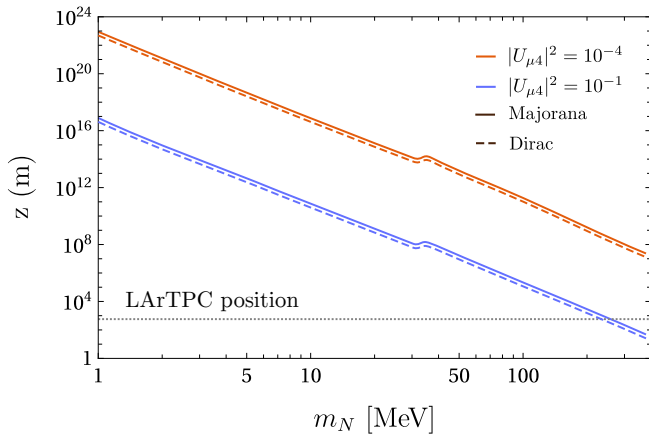


FIG. 7. Average HNL's decay positions projected along the Z axis for $|U_{\mu 4}|^2 = 10^{-4}$ and $|U_{\mu 4}|^2 = 10^{-1}$. The dotted line represents the position of the LArTPC.

V. RESULTS

A. Impact on CC events at DUNEND

As we can infer from what we have shown before, the DUNE neutrino flux fired at the DUNEND will be affected by the production of HNLs. Each HNL produced from the decay of its parent meson (or muon) replaces one active neutrino in the SM DUNE neutrino flux. In principle, there is a possibility to recover this active neutrino since the HNL can decay into one or more active ones, which, depending on their direction, could or not impact the DUNEND. However, as it is demonstrated in Fig. 7, it is unlikely that a relevant portion of these spurious active neutrinos would be created before or inside the LArTPC of the DUNEND for the mass range used in this work. This decrease in active neutrinos translates into a decrease in the CC event rates at the LArTPC. Our strategy is to use this deficit of CC events as an indirect signal of the existence(production) of HNLs at the DUNE neutrino flux. Hence, in that sense, we are conducting an indirect search for HNLs. This indirect method for searching for HNLs is complementary to the direct searches [7], which look for HNL decays inside one of the DUNE's detectors. As we will show in the following sections, our method works comparatively better than di-

rect searches for masses below 7-8 MeV and is sensitive to masses below 1 MeV, a region primarily inaccessible through direct searches.

The deficit in the total CC event rates depends on the mass of the HNL, the value of $|U_{\alpha 4}|^2$ and the off-axis position of the detector. In order to have a first estimate of the maximum significance of this deficit allowed by current limits on the mixing parameters, we calculated the active neutrino flux in presence of HNLs using the maximum values of $|U_{\alpha 4}|^2$ allowed by accelerator experiments at 90% confidence level [29] and then convoluted these fluxes with GENIE 2.8.4 [30] CC inclusive cross sections. As a point of reference, in Fig. 8 we show the ν_μ CC event rates at the LArTPC for $m_N = 1$ MeV and $|U_{\mu 4}|^2 = 1.19 \times 10^{-2}$ assuming Majorana neutrinos, on-axis position, one year in neutrino mode and $\sigma_a = 0$. The significance of the change in the number of the CC events in each bin is estimated by

$$N_\sigma = \frac{|N^{\text{BSM}} - N^{\text{SM}}|}{\sqrt{N^{\text{SM}}}} = \frac{|\Delta N|}{\sigma} \quad (14)$$

where N^{SM} represents the expected number of CC events assuming only SM interactions and N^{BSM} the number of CC events when HNLs are produced. As a first approximation, we are also ignoring all normalization uncertainties in the CC event rates, so that $\sigma = \sqrt{N^{\text{SM}}}$ is the uncertainty in each bin (which have a width of 0.5 GeV). Due to the high luminosity of the DUNE experiment, under this setup, the production of HNLs causes a decrease in the total number of CC event rates on the order of 10^5 events near 2.5 GeV. This implies a deviation from the SM prediction by approximately 40σ around this energy. This indicates that DUNE's sensitivity to $|U_{\mu 4}|^2$ might be beyond the current experimental limits for this particular HNL mass.

As the HNL mass increases, its production is suppressed, and, consequently, its presence on the active neutrino flux is reduced. As an example of the latter, we display in Fig. 9 the event rates for $m_N = 30$ MeV and the maximum value allowed for $|U_{\alpha 4}|^2$ by experiments at 90% confidence level for this mass. In this case, there is a (small) deviation, from the SM prediction, in the order of 1σ at best. This happens because of the tighter constraint on the mixing parameter.

In Fig. 10 we can see the behavior of the significance N_σ of the total deficit of ν_μ CC events at the LArTPC for a wide range of m_N , considering one year in neutrino mode and on-axis position. For each value of m_N , we fix the $|U_{\mu 4}|^2$ at its corresponding maximum allowed value at 90% confidence level. The mass dependence seen in the plot is originated by the dependence of the maximum values of $|U_{\mu 4}|^2$ on m_N . This mass dependence is absent in the flat region between 10^{-3} MeV and 1 MeV, where the mixing parameters are set to 1 since there are no accelerator-based constraints. This figure establishes that, for masses below 1 MeV, the production of HNLs

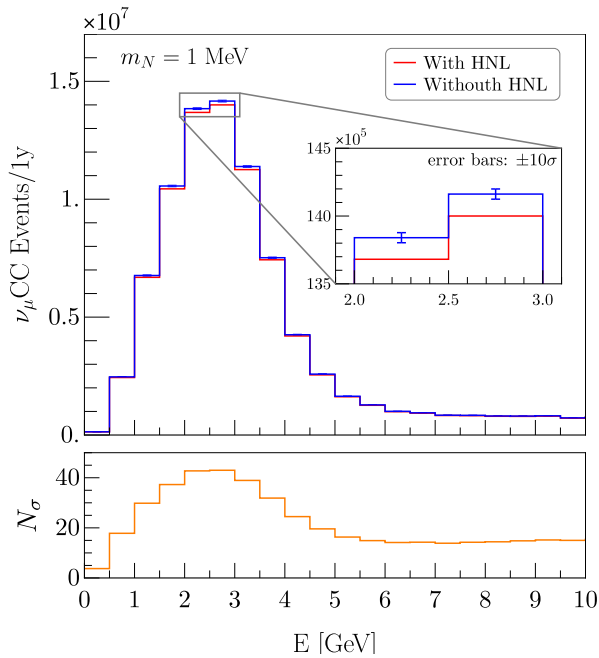


FIG. 8. ν_μ CC event rates for $m_N = 1$ MeV assuming the maximum value allowed for $|U_{\mu 4}|^2$ at 90% confidence level, on-axis position, one year in neutrino mode and $\sigma_a = 0$. The error bars are amplified by 10.

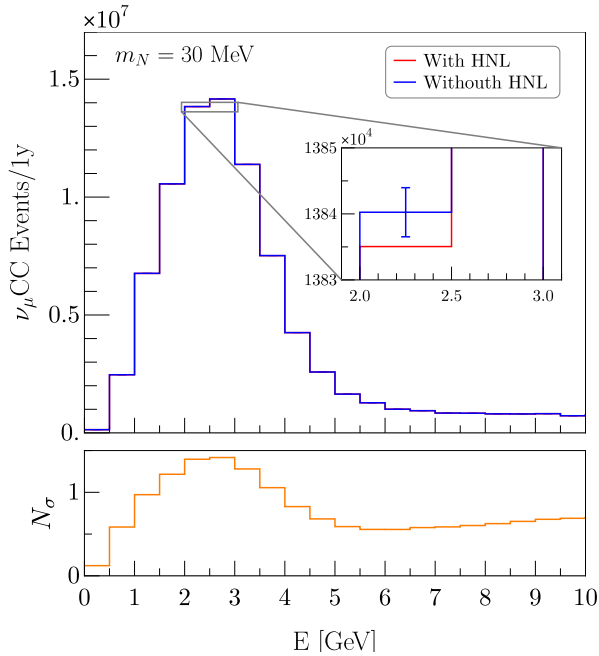


FIG. 9. ν_μ CC event rates for $m_N = 30$ MeV assuming the maximum value allowed for $|U_{\mu 4}|^2$ at 90% confidence level, on-axis position, 1 year in neutrino mode and $\sigma_a = 0$.

would be high enough for getting a deficit in the total number of CC events compatible with significances of at least 10σ . Above 10 MeV, current limits on the mixing parameters heavily suppress the possible effects of HNLs

on the number of CC events at DUNE; hence, the significance drops below 1σ , although a small region just before 100 MeV still offers a good sensitivity. Thus, DUNE will have good significance for indirect hints of the existence of low mass HNLs, such as reductions in the CC events (in comparison to expected ones).

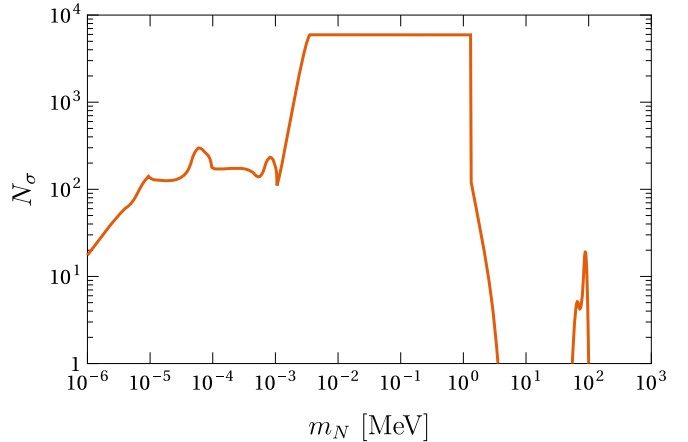


FIG. 10. Significance of the maximum possible deficit of ν_μ CC events at the LArTPC due to HNLs for $\sigma_a = 0$. Maximum values of $|U_{\alpha 4}|^2$ allowed by experiments at 90% confidence level, 1 year in neutrino mode and on-axis position were assumed.

B. Sensitivity

We estimate the sensitivity of DUNE to $(m_N, |U_{\alpha 4}|^2)$ through the following χ^2 [31]:

$$\chi^2 = \frac{a^2}{\sigma_a^2} + \frac{((1+a)N_{tot}^{BSM} - N_{tot}^{SM})^2}{N_{tot}^{SM}}, \quad (15)$$

where N_{tot}^{BSM} represents the total neutrino CC events at the LArTPC when HNLs are produced and N_{tot}^{SM} the DUNE prediction of the pure SM CC events at the LArTPC. The small parameter a encompasses the overall normalization uncertainty σ_a due to flux and cross section uncertainties. This parameter is profiled in the calculation of the χ^2 .

Our results are presented in Fig. 11. The left panel of this figure shows the estimated DUNE sensitivity to $|U_{\mu 4}|^2$ at 90% confidence level on the LArTPC assuming Majorana neutrinos, ten years of operation (five in neutrino and five in antineutrino mode) and on-axis position. In our analysis, the CC event rates from all neutrino flavors are considered (read the discussion at the end of section II). For masses below 10 MeV, the limits are independent of m_N . The latter is because of two factors. The first one is that, for these very low masses, the total number of HNLs produced is practically independent of m_N (see Fig. 5). The other factor is that the HNL lifetime for lower masses is enormous (see Fig. 7), decaying

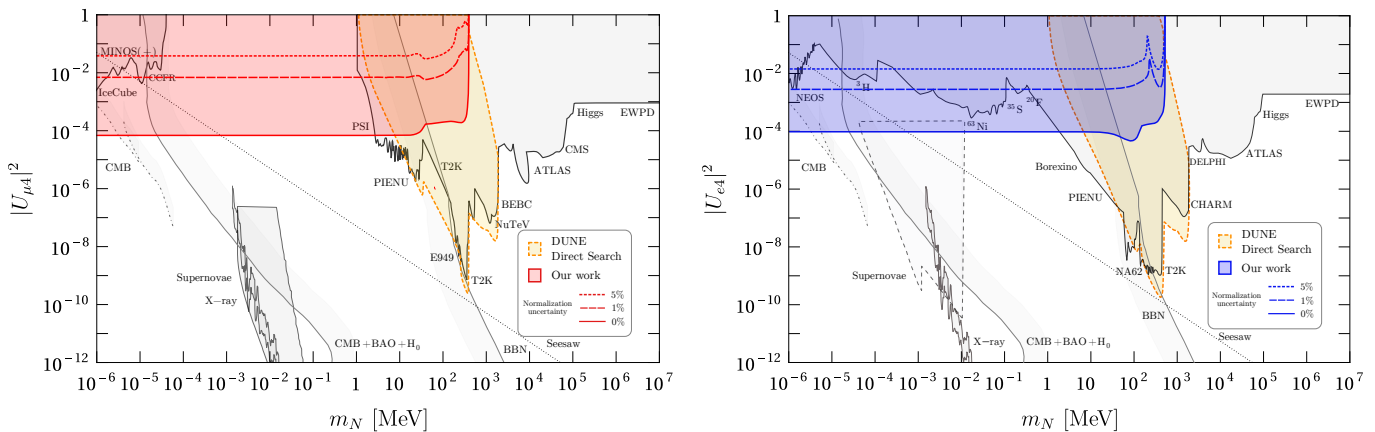


FIG. 11. Estimated limits of DUNE to $|U_{\mu 4}|^2$ (left, red) and $|U_{e 4}|^2$ (right, blue) at 90% confidence level by CC events disappearance at the LArTPC of the DUNE, for 10 years of operation (5 in neutrino and 5 in antineutrino mode) and on-axis position. The regions of experimental constraints (gray) were taken from [29, 32, 33]. The estimated sensitivity of DUNE obtained in [7] by direct searches of HNL decays is shown for comparison.

all of them far away from the detector without the possibility of leaving a trace on it. As we already know, above $m = 33.91$ MeV, the production channel $\pi^+ \rightarrow \mu^+ N$ is kinematically forbidden, and there is a sudden loss in the sensitivity. As the mass increases, production from charged kaons starts to dominate. Since charged kaons decay mostly into muon neutrinos, this translates into a small increase in sensitivity up to the end of the curve, which is at 387.81 MeV. These limits are competitive with experimental constraints below 2.5 MeV and with direct searches below 8 MeV. In particular, for $\sigma_a = 0$, below 10 MeV the limits are equal to $|U_{\mu 4}|^2 < 7 \times 10^{-5}$. These limits weaken when the value of σ_a increases. For instance, for $\sigma_a = 0.01$ and $\sigma_a = 0.05$, the sensitivity of DUNE below 10 MeV is around $|U_{\mu 4}|^2 < 7 \times 10^{-3}$ and $|U_{\mu 4}|^2 < 4 \times 10^{-2}$, respectively.

The right panel of Fig. 11 shows the expected DUNE sensitivity when we turn on $|U_{e 4}|^2$ being the other ones zero. The rest of the characteristics are the same as for the left panel. In general, the sensitivity pattern is similar to the one observed for the left panel. Below 10 MeV, most HNLs decay behind the LArTPC; hence, the sensitivity is mass-independent. Above 10 MeV, the pion decay channel $\pi^\pm \rightarrow e^\pm N$ starts to dominate because, in contrast to $\pi^\pm \rightarrow e^\pm \bar{\nu}_e$, it is less suppressed by helicity due to the larger size of the HNL mass. This effect decreases the number of both ν_e and ν_μ CC events according to the suppression factor in Eq. (12), therefore increasing the sensitivity. At around 139 MeV, HNL production from pion decays becomes kinematically forbidden, which translates into a decrease in the sensitivity. Finally, the curve ends when production from kaons is kinematically forbidden at 493.17 MeV. These limits are competitive with experimental constraints below 2.5 MeV and with direct searches below 7 MeV. In particular, for $\sigma_a = 0$, below 10 MeV the limits are equal to $|U_{e 4}|^2 < 1 \times 10^{-4}$. For $\sigma_a = 0.01$ and $\sigma_a = 0.05$, the sensitivity of DUNE below 10 MeV is around $|U_{e 4}|^2 < 3 \times 10^{-3}$

and $|U_{e 4}|^2 < 1.5 \times 10^{-2}$, respectively.

We must point out that our results are blind to the Dirac or Majorana nature of the HNL. The distinction between Dirac and Majorana HNLs is usually performed in direct searches by analyzing the distributions of charged mesons and leptons produced when the HNL decays inside the detector. We are not looking into the direct search mode since it has already been discussed in [7]. Besides their decay products, Dirac and Majorana HNLs can also be differentiated by their lifetimes due to the factor of two present in Eq. (5). However, this effect is not relevant for us because, for the mass range we studied and small mixings, almost all the HNL decays occur behind the LArTPC, as shown in Fig. 7. Furthermore, as we have discussed in section II, for very low m_N the Dirac and Majorana neutrinos are indistinguishable. Thus, we can conclude that nearly all the active neutrinos produced from the HNL decays are lost independently of the nature of neutrinos. In this way, the critical magnitude in our analysis is the production rate of HNLs, which is independent of the nature of neutrinos, so the deficit of the CC event rates is independent too. Therefore, it would not be possible to distinguish between Dirac or Majorana neutrinos through the approach presented here.

C. Off-axis sensitivity

The DUNE experiment also considers the possibility of moving the DUNE near detectors horizontally, a setup known as DUNE PRISM. We study the impact in our results of moving the LArTPC up to 30 m horizontally. We see in Fig. 12 that, for ten years of operation and $\sigma_a = 0$, the sensitivity to $|U_{\mu 4}|^2$ decreases at 30 m off-axis from $|U_{\mu 4}|^2 < 6 \times 10^{-5}$ to $|U_{\mu 4}|^2 < 3 \times 10^{-4}$. This reduction, which is about 80%, is almost the same for all

masses. We also show that, for $\sigma_a = 0.05$ (dashed line), the sensitivity becomes $|U_{\mu 4}|^2 < 2.5 \times 10^{-2}$. We conclude that, for a systematic error of 5%, this off-axis case is still competitive with direct searches below 1 MeV and with experimental constraints below 1.5 MeV.

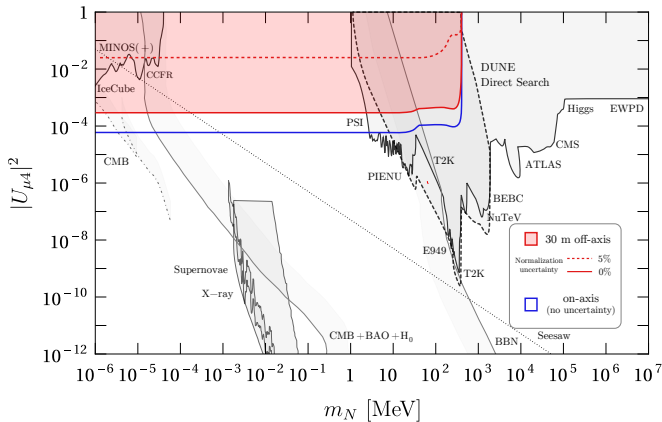


FIG. 12. Comparison between on-axis and 30 m off-axis estimated sensitivities of DUNE to $|U_{\mu 4}|^2$ at 90% confidence by neutrino CC events disappearance for 10 years of operation (5 in neutrino and 5 in antineutrino mode). The regions of experimental constraints were taken from [29, 32, 33] and the estimated sensitivity of DUNE by direct searches from [7].

D. Allowed regions for $(m_N, |U_{\alpha 4}|^2)$

We also explore the potential to constraint the $(m_N, |U_{\alpha 4}|^2)$ parameter space region in the context of this indirect search. So, assuming that the disappearance CC events are originated by the presence of HNLs within the neutrino beam, we perform a χ^2 analysis fixing our simulation in certain values of $(m_N, |U_{\alpha 4}|^2)$. The allowed regions for $m_N = 0.1$ MeV and $|U_{\mu 4}|^2 = 10^{-2}$ are presented in Fig. 13 for $\sigma_a = 0$ (red) and $\sigma_a = 0.01$ (blue). The confidence regions are bounded to the right, but extend to the left up to $m_N = 0$, a mass degeneracy that reflects the fact that our approach is not sensitive to m_N for low masses. For the ideal case $\sigma_a = 0$ (red) the 95% confidence region is sufficiently small that it is possible to constraint $|U_{\mu 4}|^2$ within an uncertainty of 10%. However, when we include systematic uncertainties (blue), we found that even for $\sigma_a = 0.01$ there is a huge degeneracy both in $|U_{\mu 4}|^2$ and m_N , a result that was expected since a 1% normalization uncertainty makes it very difficult to differentiate the effects of different points of the parameter space.

VI. CONCLUSIONS

The cornerstone of this work is to assume that the parent mesons, which products compose a neutrino

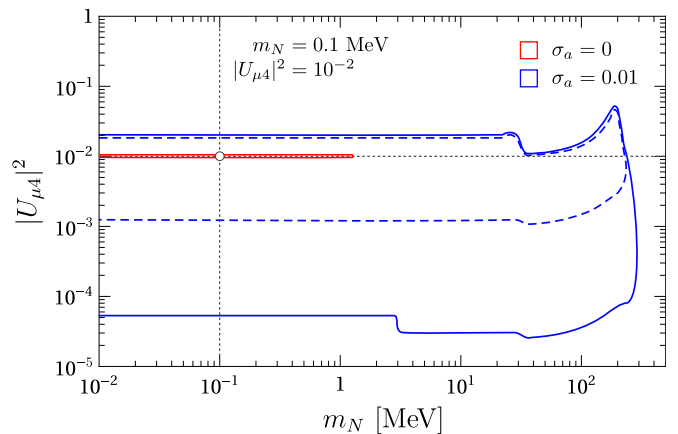


FIG. 13. χ^2 regions for 90% (dashed) and 95% (solid) confidence levels for $m_N = 0.1$ MeV, $|U_{\mu 4}|^2 = 10^{-2}$, 10 years of operation (5 in neutrino and 5 in antineutrino mode) and on axis position. The red curves represent the regions for $\sigma_a = 0$ and the blue ones for $\sigma_a = 0.01$.

beam, can decay into Heavy Neutral Leptons, resulting in the disappearance of ν_μ and ν_e CC events in the LArTPC of the DUNE. For five years per mode (neutrino/antineutrino), on-axis configuration and a (1)5% overall normalization uncertainty in the DUNE neutrino CC events, this deficit shows that DUNE will set competitive bounds of $|U_{\mu 4}|^2 < (7 \times 10^{-3})4 \times 10^{-2}$ and $|U_{e 4}|^2 < (3 \times 10^{-3})1.5 \times 10^{-2}$ for masses below 1.5 MeV. These limits are better than the ones predicted by DUNE direct searches or even placed in mass regions inaccessible to them. These bounds are still competitive for the off-axis configuration. Besides, we explore the capacity of determining the allowed parameter space region $(m_N, |U_{\alpha 4}|^2)$ for some specific pair values, obtaining uncertainties in the order of 10% for $m_N = 0.1$ MeV and $|U_{\mu 4}|^2 = 10^{-2}$ when we ignore the systematic uncertainties; however, for a systematic uncertainty of 1%, we found that the degeneracy is too large to reliably constraint the values of $(m_N, |U_{\mu 4}|^2)$. Finally, it is worth noting that the disappearance of CC events as a HNL signature is complementary to the direct observation or HNL decays, showing an attractive potential to be used in neutrino Near Detectors with high ν CC event rates.

ACKNOWLEDGMENTS

A. M. G. acknowledges funding by the Dirección de Gestión de la Investigación at PUCP, through grants No. DGI-2017-3-0019 and No. DGI 2019-3-0044. S. C. acknowledges CONCYTEC for the graduate fellowship under Grant No. 236-2015-FONDECYT. The authors also want to thank Zarko Pavlovic for useful remarks regarding the interpretation of the BIWG data, Margot Delgado de la Flor for her help at the initial stages of this work and R. E. Shrock, C. Argüelles, I. Shoemaker, A. de Roeck, O. Peres and W. Rodejohann for their useful

remarks on our first manuscript.

-
- [1] M. Drewes, The Phenomenology of Right Handed Neutrinos, *Int. J. Mod. Phys. E* **22**, 1330019 (2013).
- [2] A. Atre, T. Han, S. Pascoli, and B. Zhang, The Search for Heavy Majorana Neutrinos, *JHEP* **05**, 030.
- [3] S. F. King, Neutrino mass models, *Rept. Prog. Phys.* **67**, 107 (2004).
- [4] M. Drewes *et al.*, A White Paper on keV Sterile Neutrino Dark Matter, *JCAP* **01**, 025.
- [5] S. Davidson, E. Nardi, and Y. Nir, Leptogenesis, *Phys. Rept.* **466**, 105 (2008).
- [6] K. N. Abazajian *et al.*, Light Sterile Neutrinos: A White Paper, (2012), [arXiv:1204.5379 \[hep-ph\]](https://arxiv.org/abs/1204.5379).
- [7] J. M. Berryman, A. de Gouvea, P. J. Fox, B. J. Kayser, K. J. Kelly, and J. L. Raaf, Searches for Decays of New Particles in the DUNE Multi-Purpose Near Detector, *JHEP* **02**, 174.
- [8] R. E. Shrock, New Tests For, and Bounds On, Neutrino Masses and Lepton Mixing, *Phys. Lett. B* **96**, 159 (1980).
- [9] R. E. Shrock, General Theory of Weak Leptonic and Semileptonic Decays. 1. Leptonic Pseudoscalar Meson Decays, with Associated Tests For, and Bounds on, Neutrino Masses and Lepton Mixing, *Phys. Rev. D* **24**, 1232 (1981).
- [10] A. Aguilar-Arevalo *et al.* (PIENU), Search for heavy neutrinos in $\pi \rightarrow \mu\nu$ decay, *Phys. Lett. B* **798**, 134980 (2019).
- [11] Artamonov *et al.* (E949 Collaboration), Search for heavy neutrinos in $K^+ \rightarrow \mu^+\nu_H$ decays, *Phys. Rev. D* **91**, 052001 (2015).
- [12] B. Abi *et al.* (DUNE), Deep Underground Neutrino Experiment (DUNE), Far Detector Technical Design Report, Volume I Introduction to DUNE, *JINST* **15** (08), T08008.
- [13] B. Abi *et al.* (DUNE), Deep Underground Neutrino Experiment (DUNE), Far Detector Technical Design Report, Volume II: DUNE Physics, (2020), [arXiv:2002.03005 \[hep-ex\]](https://arxiv.org/abs/2002.03005).
- [14] C. Giganti, S. Lavignac, and M. Zito, Neutrino oscillations: The rise of the PMNS paradigm, *Prog. Part. Nucl. Phys.* **98**, 1 (2018).
- [15] M. Gronau, C. N. Leung, and J. L. Rosner, Extending Limits on Neutral Heavy Leptons, *Phys. Rev. D* **29**, 2539 (1984).
- [16] K. Bondarenko, A. Boyarsky, D. Gorbunov, and O. Ruchayskiy, Phenomenology of GeV-scale Heavy Neutral Leptons, *JHEP* **11**, 032.
- [17] J. D. Richman and P. R. Burchat, Leptonic and semileptonic decays of charm and bottom hadrons, *Rev. Mod. Phys.* **67**, 893 (1995).
- [18] P. Ballett, T. Boschi, and S. Pascoli, Heavy Neutral Leptons from low-scale seesaws at the DUNE Near Detector, *JHEP* **03**, 111.
- [19] A. Abada, D. Bečirević, O. Sumensari, C. Weiland, and R. Z. Funchal, Sterile neutrinos facing kaon physics experiments, *Phys. Rev. D* **95**, 075023 (2017).
- [20] B. Kayser and R. E. Shrock, Distinguishing Between Dirac and Majorana Neutrinos in Neutral Current Reactions, *Phys. Lett. B* **112**, 137 (1982).
- [21] A. Abed Abud *et al.* (DUNE), Deep Underground Neutrino Experiment (DUNE) Near Detector Conceptual Design Report, *Instruments* **5**, 31 (2021).
- [22] DUNE Collaboration, <http://home.fnal.gov/~ljf26/DUNEFluxes/>.
- [23] S. Agostinelli *et al.* (GEANT4), GEANT4—a simulation toolkit, *Nucl. Instrum. Meth. A* **506**, 250 (2003).
- [24] J. Allison *et al.*, Recent developments in Geant4, *Nucl. Instrum. Meth. A* **835**, 186 (2016).
- [25] A. Ferrari, P. R. Sala, A. Fasso, and J. Ranft, FLUKA: A multi-particle transport code (Program version 2005) [10.2172/877507](https://arxiv.org/abs/10.2172/877507) (2005).
- [26] T. T. Böhlen, F. Cerutti, M. P. W. Chin, A. Fassò, A. Ferrari, P. G. Ortega, A. Mairani, P. R. Sala, G. Smirnov, and V. Vlachoudis, The FLUKA Code: Developments and Challenges for High Energy and Medical Applications, *Nucl. Data Sheets* **120**, 211 (2014).
- [27] T. Sjöstrand, S. Ask, J. R. Christiansen, R. Corke, N. Desai, P. Ilten, S. Mrenna, S. Prestel, C. O. Rasmussen, and P. Z. Skands, An introduction to PYTHIA 8.2, *Comput. Phys. Commun.* **191**, 159 (2015).
- [28] B. Abi *et al.* (DUNE), Experiment Simulation Configurations Approximating DUNE TDR, (2021), [arXiv:2103.04797 \[hep-ex\]](https://arxiv.org/abs/2103.04797).
- [29] P. D. Bolton, F. F. Deppisch, and P. S. Bhupal Dev, Neutrinoless double beta decay versus other probes of heavy sterile neutrinos, *JHEP* **03**, 170.
- [30] C. Andreopoulos *et al.*, The GENIE Neutrino Monte Carlo Generator, *Nucl. Instrum. Meth. A* **614**, 87 (2010).
- [31] I. Bischer and W. Rodejohann, General Neutrino Interactions at the DUNE Near Detector, *Phys. Rev. D* **99**, 036006 (2019).
- [32] D. A. Bryman and R. Shrock, Improved Constraints on Sterile Neutrinos in the MeV to GeV Mass Range, *Phys. Rev. D* **100**, 053006 (2019).
- [33] C. A. Argüelles, N. Foppiani, and M. Hostert, Heavy neutral leptons below the kaon mass at hodoscopic neutrino detectors, *Phys. Rev. D* **105**, 095006 (2022).